pH-Modulated Pigment Antenna in Lipid Bilayer on Photosensitized Semiconductor Electrode

Peter Fromherz* and Wolfgang Arden

Contribution from the Max-Planck-Institute of Biophysical Chemistry, Department of Development of Molecular Systems, D-34 Goettingen-Nikolausberg, Germany.
Received March 21, 1980

Abstract: The chemical synthesis and physical analysis of a molecular device are described, where in a reaction sequence protons, photons, and electrons are involved. A bimolecular membrane of docosylamine is deposited onto an indium–tin oxide electrode. The bilayer is doped on one side by a cyanine pigment in direct contact with the semiconductor and on the other side by a coumarin pigment in contact with the electrolyte. The absorption spectrum of the coumarin depends on pH. The fluorescence spectrum overlaps with the absorption of the cyanine. The oxidation potential of the excited cyanine is in the range of the conduction band of indium–tin oxide. Spatial order and energetic matching are the basis of a reaction sequence: pH enhances dissociation of the coumarin, which leads to enhanced excitation in the tuned incident light. Deexcitation of the antenna pigment and excitation of the cyanine by energy transfer produces electron transfer to the surface of the semiconductor. The charge is separated by the field in the Schottky layer and observed as photocurrent. The sequential energy and electron transfer leads to an imaging of the chemical features of the coumarin onto the semiconductor. The structure and mechanism of the device are characterized by spectroscopic and electrochemical methods. The particular role of pH-dependent electrical potentials at the surface of membrane and electrode is investigated.

I. Introduction

A pigment may be excited by electromagnetic energy transfer from an antenna dye as excited by external illumination.[1] The process requires for the donor tuning of its absorption band to the wavelength of incident light, high yield of emission, and good spectral overlap of its emission band with the absorption of the acceptor.[2] Reversible physical or chemical modification of the donor such that these parameters are changed modulates energy transfer and leads consequently to a modulation of acceptor excitation and of all reactions originating in that excited pigment.

Such chemical sensitization by energy transfer has been verified in a previous paper with a pH-sensitive donor, modulating the fluorescence of an acceptor, both components being separated by a lipid bilayer.[3] The emission of the acceptor reflected the chemical features of the donor in all details, its titration curve and the pK shifts caused by electrical potentials at the membrane surface.[4] The electromagnetic interaction does not only transfer energy, but channels chemical information from one side of the membrane—as probed by the antenna pigment—to the other side, as detected by the photoprocess of the reaction pigment.

The bilayer arrangement has been deposited onto a semiconductor electrode, such that the excited acceptor pigment transfers an electron to the conduction band as detected by photocurrent measurement.[5] The effect of an antenna onto that reaction is revealed by the action spectrum of the sensitized photocurrent, which indicated a successful transfer of energy and electron in a sequence.[6]

The present paper describes the realization of a pH-modulated antenna with subsequent energy and electron transfer. The system is assembled in a lipid bilayer between electrolyte and semiconductor. The structure and mechanism of the device are shown in Figure 1.[7] The overall functional realization of the project is demonstrated first. Then, after a description of experimental set-up and of theoretical relations on interfacial acid–base equilibria, a detailed analysis of the structure and mechanism is presented: of bilayer, pH-sensitive antenna, semiconductor, electron injection from reaction pigment, and the complete proton-switched energy-electron-transfer device.

The main purpose of the paper is not the investigation of a novel physico-chemical elementary process. The issue is chemical synthesis and physical characterization of an artificial device where the molecular components are coupled in a way that a sequence of reactions is opened as envisaged a priori on the basis of the nature of the components.[8] The work presented here is part of a more involved design, where the antenna is switched internally by local catalysis of a membrane-bound enzyme,[9] such that intermolecular couplings by proton, photon, and electron are integrated.[7]

II. The Function

The components of the molecular device are as follows (Figure 1B). The backbone is a bimolecular layer of docosylamine. The pH-sensitive antenna is a coumarin (I). The redox pigment is a cyanine (II). The electrode is a thin film of indium–tin oxide. The electrolyte is an aqueous solution of 10 mM sodium citrate, 18 mM Tris, and 1.5 M thiourea.

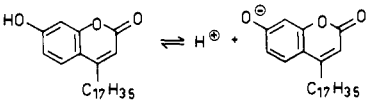

I

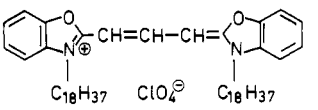

II

The energetics is shown in Figure 2. The oxidation potential R^*/R^+ of the excited reaction pigment is well in the range of the conduction band of the semiconductor, taking into account that the band structure is shifted by about −59 mV per pH unit under condition of constant space charge. The emission of the antenna A/B matches the absorption of the acceptor R. The absorption energy of the antenna is lowered by dissociation of a proton. This leads to a match with the quantum energy of incident light. The pK of the antenna is in the neutral pH range.

The actual function of the device is shown in Figure 3. The upper trace reflects the steps in photocurrent across the elec-

(1) J. Perrin, Deuxieme Conseil de Chimie Solvay, Bruxelles, 1925, Gauthier-Villars, Paris, 1926, p 322.
(2) T. Foerster, *Ann. Phys.* **2**, 55 (1948).
(3) P. Fromherz, *Chem. Phys. Lett.*, **26**, 221 (1974).
(4) P. Fromherz, *Biochim. Biophys. Acta*, **323**, 326 (1973).
(5) W. Arden and P. Fromherz, *J. Electrochem. Soc.*, **127**, 370 (1980).
(6) W. Arden and P. Fromherz, *Ber. Bunsenges. Phys. Chem.*, **82**, 871 (1978).
(7) P. Fromherz, Habilitationsschrift, University of Marburg, 1977.
(8) H. Kuhn, *Verh. Schweiz. Naturforsch. Ges.*, 245 (1965).
(9) P. Fromherz in "Regular 2D-Arrays of Biomacromolecules", W. Baumeister, Ed., Springer, Berlin, 1980.

0002-7863/80/1502-6211$01.00/0

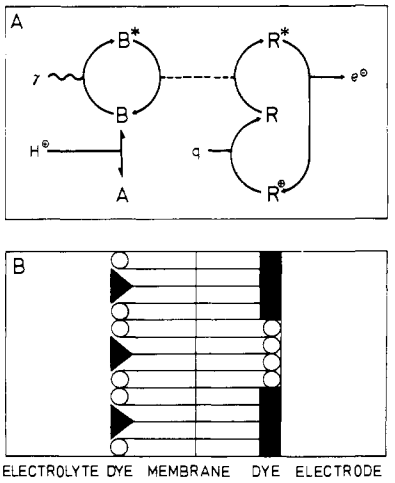

Figure 1. Structure and mechanism of the pH-modulated energy–electron-transfer device. A and B are acidic and basic forms of the antenna pigment (coumarin). R is the reaction pigment (cyanine), accepting energy from the antenna and injecting an electron into the conduction band of the semiconductor. γ denotes incident light; q is an external reductant.

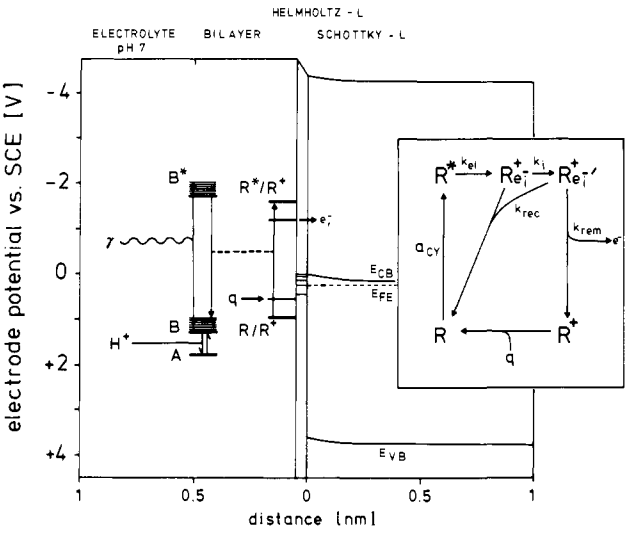

Figure 2. Energy diagram of the components. Band structure and oxidation potentials are referred to the saturated calomel electrode (SCE). The scheme is drawn for pH 7 and an applied potential of +150 mV above the flatband potential (V_{FB} = +170 mV). E_{VB}, E_{CB}, and E_{FE} are the energies of valence and conduction band and of the Fermi level. The absolute levels of the antenna dye are arbitrary. The construction of the diagram is described in the text. The insert shows the reaction sequence for electron injection. $R^+e_i^-$ and $R^+e_i^{-\prime}$ are intermediates formed by electron transfer. The notation of rate constants is given in the text.

trode/electrolyte interface when the pH is changed from 6 to 8. This overall input–output effect is the result of the following chain of molecular events (Figure 1A): enhancement of antenna dissociation, excitation of antenna base by incident light, deactivation of antenna and excitation of reaction pigment, oxidation of that pigment by the conduction band, and removal of the transferred electron by the space charge to the bulk of the semiconductor. The whole switching is reversible as indicated in Figure 3. The conditions of the experiment are chosen such that the redox reaction is pH independent as indicated by the lower trace in Figure 3, where the cyanine is excited directly.

III. Materials and Methods

1. Electrode. The electrode is made from indium–tin oxide (Merck) by thermal evaporation under high vacuum on a glass slide and reoxidation at 400 °C. The material consists of 70% In and 30% Sn.[5] The thickness is 30 nm, the conductivity 30–300 S/cm, and the Hall mobility 10–20 $cm^2/(V\ s)$. A dielectric constant of 6 is assumed.[10,11] The energy

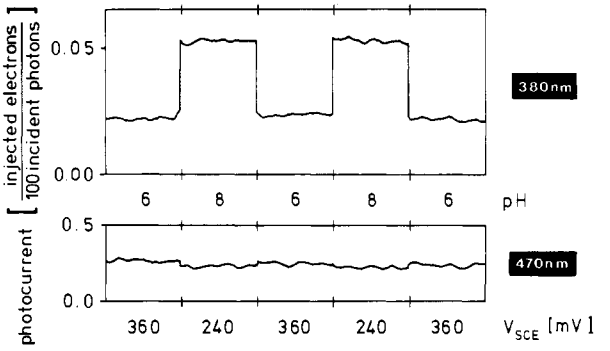

Figure 3. Input–output function of the pH-modulated energy–electron-transfer device. The upper trace is the photocurrent with illumination of the antenna pigment at 380 nm, the lower trace with illumination of the reaction pigment at 470 nm. The switching from pH 6 to 8 is made under constant-field conditions in the space charge. The pH-dependent Helmholtz potential is followed by the applied potential (−60 mV/pH unit).

levels shown in Figure 2 are calculated with an electron affinity of 4.4 eV,[12] a band gap of 3.6 eV,[11] an energy of saturated calomel electrode (SCE) vs. vacuum of 4.75 eV,[13] and a flatband potential at pH 7 of +170 mV (section VC).

The electrochemical cell is a cylindrical boring (diameter 8 mm, depth 15 mm) in a block of black PVC, which is closed by the slide carrying the electrode as contacted by indium solder. The standard composition of the electrolyte is 10 mM tris(hydroxymethyl)aminomethane (Tris), 1.5 M thiourea with 30 mM NaCl, or 10 mM sodium citrate. It is contacted by a saturated calomel electrode. The pH is adjusted with NaOH and HCl. The solution may be exchanged during the photoelectrochemical measurements.

2. Bilayer. The bimolecular membrane is deposited onto the electrode by transferring monomolecular films from the air–water interface.[14] The monolayers are spread from a 5 mM solution of docosylamine (Merck, recrystallized) in chloroform/methanol (10:1) and transferred from a subphase of pH 9 at a surface pressure of 40 dyn/cm and a speed of 1 cm/min, using an automatic surface pressure controlled trough and a precision transferring lift.[15] The electrode/membrane assembly is kept in contact with water during all manipulations necessary for mounting of the electrode.[15] Doping of the monolayers by chromophores is achieved by mixing of the solutions before spreading.[16]

The antenna dye is a hydroxycoumarin (I). It is applied at molar ratios with docosylamine of 40:100 and 0.5:100. With excitation in the absorption maximum of the base the fluorescence intensity is proportional to the dissociation degree of the chromophore bound to the lipid film.[4] The photosensitizer is a cyanine (II).[17] It is applied at a molar ratio of 20:100 with docosylamine. The oxidation potential of the ground state is 0.94 V and that of the excited singlet state 1.62 V.[18] The Franck–Condon shifts for electron donation and acceptance as indicated in Figure 2 are assumed to be 0.4 eV.[19] Note that the absolute location of the energy levels of the antenna dye in Figure 2 is arbitrary.

3. Measurements. The capacitance of the electrode without and with bilayer is measured in a three-electrode configuration with a platinum counterelectrode. The probe ac has an amplitude of 10 mV and an angular frequency of 1 kHz. Finite conductivities of electrode and electrolyte are compensated (potentiostat PAR 173/176).

The illumination of the electrode is provided by a 200-W xenon lamp through a monochromator and a chopper of 2 Hz. The intensity at 470 nm is 100 $\mu W/cm^2$ at a band width of 5 nm. The photocurrent is obtained from a current–voltage converter holding the electrolyte on virtual ground. The electrode potential is applied by a battery. The chopped signal is corrected by differentiation and amplified by a lock-in

(10) H. J. van Daal, *J. Appl. Phys.*, **39**, 4467 (1968).
(11) H. K. Mueller, *Phys. Status Solidi*, **27**, 723 (1968).
(12) E. Wang and L. Hsu, *J. Electrochem. Soc.*, **125**, 1328 (1978).
(13) F. Lohmann, *Z. Naturforsch.*, **22a**, 843 (1967).
(14) K. B. Blodgett, *J. Am. Chem. Soc.*, **57**, 1007 (1935).
(15) P. Fromherz, *Rev. Sci. Instrum.*, **46**, 1380 (1975).
(16) H. Kuhn, D. Moebius, and H. Buecher in "Physical Methods of Chemistry", Vol. 1, Part 3B, A. Weissberger and B. W. Rossiter, Eds., Wiley, New York, 1972, p 577.
(17) J. Sondermann, *Justus Liebigs Ann. Chem.*, **749**, 183 (1971).
(18) R. F. Large in "Photographic Sensitivity", R. J. Cox, Ed., Academic Press, London, 1973, p 241.
(19) H. Gerischer and F. Willig, *Top. Curr. Chem.*, **61**, 31 (1976).

technique. Fluorescence is detected by a photomultiplier through a second monochromator. Excitation and emission spectra are plotted and corrected for incident quantum flux and detection characteristics, respectively.

IV. Interfacial Acid–Base Equilibria

The following sections are concerned with acid–base reactions at surfaces and their interference with interfacial electrical charge density and potential. Since no unequivocal representation of the relevant relations is available, the next section describes the essential formulas for reference purposes.

1. Equilibrium Condition. The electrochemical equilibrium of any acid–base reaction $xA_x^m = B_x^m + H^+$, where A_x^m and B_x^m are functional groups fixed in an interfacial medium m and where the proton H^+ is in equilibrium with the bulk water phase, is described by eq 1 with b_x the fraction of base and $\Phi_{th} = kT/e$

$$\log \frac{b_x}{1 - b_x} = pH^w - pK_x^i + \Psi/2.3\Phi_{th} \qquad (1)$$

= 25 mV at room temperature (e = proton charge, kT = thermal energy). pK_x^i is the interfacial pK, i.e., the pK of dissociation of interfacial acid into interfacial base and aqueous proton without interference of electrical potential.[20] pH^w is the pH of the bulk water phase. The electrical interfacial potential Ψ as referred to the bulk water phase may originate from dipoles (Ψ_0) and from an electrical charge density s as contributing to potential by a double layer relation $\Phi(s)$ (eq 2). The charge density s is the

$$\Psi = \Psi_0 + \Phi(s) \qquad (2)$$

sum of permanent charges s_0 and the charges of all acid–base reactions x according to eq 3, where n_x is the density of functional group x, z_x^A and z_x^B are the charge numbers of acid and base, and the b_x are determined by eq 1.

$$s = s_0 + \sum_x [z_x^A(1 - b_x) + z_x^B b_x] e n_x \qquad (3)$$

The pH^w for semidissociation ($b_x = {}^1/_2$) is denoted by pK_x^{mw} as defined by eq 4, where $\Psi_{x/2}$ is the electrical potential for b_x

$$pK_x^{mw} = pK_x^i - \psi_{x/2}/2.3\Phi_{th} \qquad (4)$$

$= {}^1/_2$. If Ψ is independent of b_x and pH^w, eq 1 is an ideal titration curve with a pK of $pK_x^{mw} = pK_x^i - \Psi/2.3\Phi_{th}$. In this form it has been applied for the evaluation of pH indicator titration in micelles.[20] Note that pK^i and pK^{mw} have to be distinguished clearly from the pK's of reaction x within a homogeneous phase of water or a nonaqueous medium, pK^w and pK^m.[20]

2. pH Dependence of Dissociation and Potential. In general the equilibrium shift of an interfacial acid–base reaction as induced by pH modifies the charge density (eq 3) and leads to a change of potential with pH (eq 2) and to a deformation of the titration curve.[21] The slopes ds/dpH and $d\Psi/dpH$ are given by eq 5 and 6 as obtained by differentiation of eq 2 and 3.

$$\frac{ds}{dpH^w} = \left(\frac{\partial s}{\partial pH^w}\right)_\Psi \left[1 - \left(\frac{\partial s}{\partial \Psi}\right)_{pH} \Big/ \frac{ds}{d\Psi}\right]^{-1} \qquad (5)$$

$$\frac{d\Psi}{dpH^w} = \left(\frac{\partial \Psi}{\partial pH^w}\right)_s \left[1 - \left(\frac{\partial \Psi}{\partial s}\right)_{pH} \Big/ \frac{d\Psi}{ds}\right]^{-1} \qquad (6)$$

$d\Psi/ds$ is the slope of the double layer (eq 2). $(\partial s/\partial\Psi)_{pH}$ is the electrochemical polarizability, which has a negative sign. The slope of the charge titration curve ds/dpH^w approaches the ideal value $(\partial s/\partial pH^w)_\Psi$ for a soft double layer, i.e., small $d\Psi/ds$. The potential change per pH unit $d\Psi/dpH$ approaches the limit $(\partial\Psi/\partial pH^w)_s = -2.3\Phi_{th}$ for a hard double layer, i.e., large $d\Psi/ds$.

The quantities as applied in subsequent sections are the width of a titration curve $w_x \equiv (dpH/db_x)$ at $b_x = 0.5$ and the ratio of $2.3\Phi_{th} = 59$ mV and $-d\Psi/dpH \equiv \Phi_{pH}$. If only one acid–base reaction x is considered, the evaluation of eq 5 and 6 with eq 1, 2, and 3 leads to eq 7 and 8. $\delta s_x = e(z_x^A - z_x^B)n_x$ is the increment

$$w_x = 1.75\left[1 + \frac{\delta s_x}{4\Phi_{th}} \frac{d\Phi}{ds}\right] \qquad (7)$$

$$\frac{2.3\Phi_{th}}{\Phi_{pH}} = \left[1 + \frac{1}{b_x(1 - b_x)} \frac{\Phi_{th}}{\delta s_x} \frac{ds}{d\Phi}\right] \qquad (8)$$

of charge density by reaction x. Further evaluation of eq 7 and 8 requires an explicit expression for the double layer relation $\Phi(s)$ or $d\Phi/ds$, respectively.

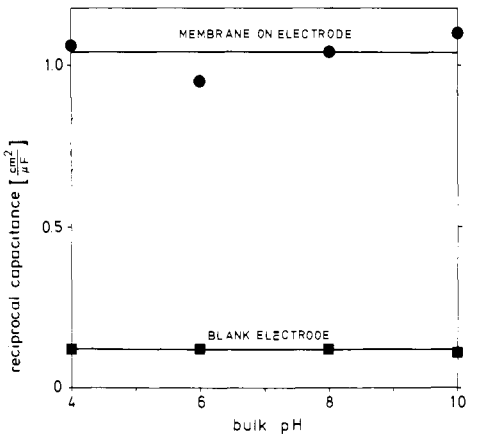

Figure 4. Reciprocal effective capacitance of the electrode without and with deposited bilayer as a function of pH. The data refer to a potential 120 mV below the flatband potential.

V. Structure and Mechanism

A. Bilayer. This section describes the chemical and physical state of the bimolecular layer of docosylamine on the indium–tin oxide electrode, i.e., its protonation and perforation.

1. Structure and Capacitance. The capacitance of the electrode C_{EL} is lowered by deposition of a bilayer. The increase of reciprocal effective capacitance C_{eff}^{-1} is shown in Figure 4 under potential conditions without space charge in the semiconductor. The increment of C_{eff}^{-1} is smaller than to be expected from the capacitance C_{BL} of an ideal bilayer of docosylamine. Figure 4 indicates $C_{eff}^{-1} - C_{EL}^{-1} = 0.92$ cm$^2/\mu$F. From multibilayers of cadmium arachidate and cadmium behenate in wet and dry systems,[5,22] one estimates for docosylamine $C_{BL}^{-1} = 2.86$ cm$^2/\mu$F.

The smaller increment may be due to four types of structural defects of the bilayer: (a) reduced thickness due to inclined molecules, (b) reduced electrical thickness due to penetration of electrolyte, (c) loosely packed films with low parallel resistance, and (d) perforation by holes with direct contact of electrode and electrolyte. The unique feature of the semiconductor substrate is its capacitance modulation by potential due to the changing space charge (cf. eq 14). This opens a way for discrimination of structure d from structure a to c. For the homogeneous models the increment of C_{eff}^{-1} due to the bilayer is independent of the capacitance of the substrate, whereas for the inhomogeneous model the increment varies with C_{EL}. It approaches the ideal value C_{BL} for low C_{EL}. It has been shown that only model d explains the potential-dependent capacitance of a bilayer coated electrode.[5]

The effective capacitance of the electrode with inhomogeneous dielectric is expressed by the capacitance of electrode and of ideal bilayer and by the fraction of holes h according to eq 9.[5]

$$\frac{1}{C_{eff}} = \left[\frac{1}{1 + h(1 + C_{EL}/C_{BL})}\right]\left[\frac{1}{C_{BL}} + \frac{1}{C_{El}}\right] \qquad (9)$$

Evaluation of Figure 4 with eq 9, assuming for the bilayer capacitance the ideal value, leads to a hole fraction of $h = 0.08$ independent of pH. This effective perforation is assigned to

(20) M. S. Fernandez and P. Fromherz, *J. Phys. Chem.*, **81**, 1755 (1977).
(21) T. A. J. Payens, *Philips Res. Rep.*, **10**, 425 (1955).
(22) B. Mann and H. Kuhn, *J. Appl. Phys.*, **42**, 4398 (1971).

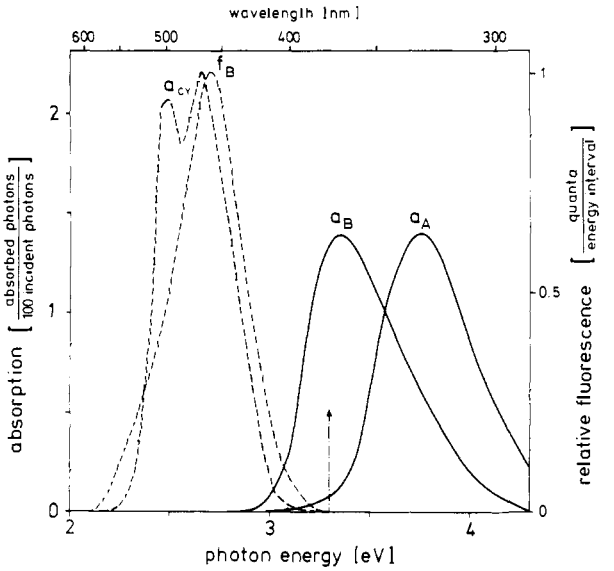

Figure 5. Absorption spectra (pH 5, a_A and pH 9, a_B) and fluorescence spectrum (f_B) of coumarin pigment (I) in docosylamine (molar ratio 40:100) and absorption spectrum (a_{CY}) of cyanine pigment (II) in docosylamine (molar ratio 20:100). The excitation energy for pH switching is marked with an arrow.

roughness of the electrode. It is higher than that found for a cadmium arachidate bilayer,[5] which may be due to the high stiffness of the docosylamine monolayer on the water surface during deposition.

2. Protonation of the Amine Matrix. The pK of long-chain amine in water is $pK^w_{AM} = 10.6$.[23] Assuming that location in the membrane structure leads to a downward shift by about one unit,[20] the interfacial pK is $pK^i_{AM} = 9.5$. The observable pK^{mw}_{AM} is obtained with the electrical potential $\Psi_{AM/2}$ for semiprotonated amine membrane according to eq 4.

The electrical potential at positively charged monolayers may be described satisfactorily by the Gouy–Chapman relation $\Psi = \Phi_{GC}(s)$ as expressed by eq 10.[24,25] c and z are concentration and

$$\Phi_{GC} = (2\Phi_{th}/|z|)\ \sinh^{-1}(s/s_{th});\ s_{th} = \sqrt{8\epsilon kTc} \qquad (10)$$

charge number of the counterions; ϵ is the permittivity of water. With a value of $s/e = 2.5 \times 10^{14}$ cm^{-2}, half of the density of a condensed docosylamine monolayer, one obtains from eq 10 for 10 mM citrate ($z = -3$) $\Psi = +70$ mV and for 40 mM chloride (NaCl and Tris) $\Psi = +175$ mV. The estimates are supported by potential measurements with the pH indicator under conditions of full amine protonation as discussed in the next section. The pK of the amine membrane is obtained from eq 4: for citrate $pK^{mw}_{AM} = 8.3$ and for chloride $pK^{mw}_{AM} = 6.5$.

The width of matrix titration is obtained from eq 7. Considering that $en_{AM} \gg s_{th}$, the slope $ds/d\Phi$ for a Gouy–Chapman layer is approximated by eq 11 and the width is given then by eq 12.

$$ds/d\Phi_{GC} = |z|\cdot|s|/2\Phi_{th} \qquad (11)$$

$$w_x = 1.75\left[1 + \frac{\delta s_x/2}{|z|\cdot|s|}\right] \qquad (12)$$

Since the protonated amine is the only charged group, one has $|s| = \delta s_x/2 = en_{AM}/2$. The ideal width of 1.75 is broadened in citrate to $w_{AM} = 2.3$ and in chloride to $w_{AM} = 3.5$. Thus the deprotonation range of the membrane is about 7.2 to 9.4 with 10 mM citrate and 4.8 to 8.2 with 40 mM chloride.

B. Antenna Pigment. This section describes the spectral and chemical features of the coumarin dye, its absorption and fluorescence, and its titration at low and high density in the docosylamine matrix.

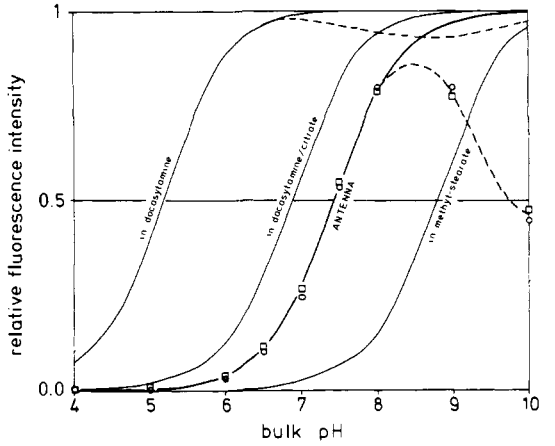

Figure 6. Fluorescence titration of coumarin dye (I) in various monolayers. The points refer to the antenna configuration (molar ratio with docosylamine 40:100, 10 mM sodium citrate) (○) with acceptor pigment and (□) without acceptor divided by a factor of 2. The other three titration curves refer to low indicator density (molar ratio 0.5:100), from right to left in methyl stearate, in docosylamine with 10 mM sodium citrate, and in docosylamine with 30 mM NaCl.

1. Absorption and Emission. The absorption of a docosylamine monolayer doped with the coumarin dye at a molar ratio 40:100 is shown in Figure 5 for full protonation and deprotonation. The shift of absorption of the base to longer wavelength is as in aqueous solution.[26] The relative amplitudes are somewhat changed. The data of Figure 5 represent $(1 - T)$ (T = transmission) of the dye–bilayer–glass system as referred to the same system without dye, i.e., disregarding corrections due to interference effects.[27] The fluorescence spectrum is identical for acid and base, owing to the strong acidic nature of the excited state.

2. pH Indicator Titration. The pK of the coumarin in the docosylamine membrane at high dilution (molar ratio 0.5:100) is $pK^{mw}_{CM} = 6.9$ with citrate and $pK^{mw}_{CM} = 5.2$ with chloride as shown in Figure 6. The interfacial pK in monolayers and micelles is $pK^i_{CM} = 8.8$, as indicated in Figure 6.[4,20] (The pK in water is $pK^w_{CM} = 7.7$.) The shift of the titration curve indicates an electrical potential according to eq 4.[20] For citrate one obtains $\Psi = +110$ mV and for chloride $\Psi = +210$ mV.

The electrical potentials in docosylamine as determined by the indicator method correspond closely to theoretical values calculated as in the previous section with the Gouy–Chapman equation, assuming full protonation of the amine matrix. With $s = en_{AM} = 5 \times 10^{14}$ e/cm^2 one obtains from eq 10 for citrate $\Psi = +100$ mV and for chloride $\Psi = +210$ mV. The deviation of the titration curve from ideal shape in chloride above pH 7 (Figure 6) indicates the onset of matrix deprotonation in that case.

3. Antenna Titration. Titration of the coumarin dye at high doping density in docosylamaine (molar ratio 40:100) is shown in Figure 6. The increase of fluorescence around pH 7 is followed by a decrease around pH 9. Introduction of the energy acceptor into the assembly reduces the fluorescence intensity by a factor of 2 without changing the shape of the titration curve.

The low-pH parts of the experimental data are fitted by an ideal titration curve with pK = 7.4. The high density of dye leads to a pK shift due to the contribution of the negative charges of the dye itself. With the Gouy–Chapman theory one obtains for semiprotonated pigment in fully protonated matrix with eq 3 and 10 $\Psi = +70$ mV, i.e., a shift by half a pH unit as compared to the low pigment density. Despite the high density of dissociable groups, broadening of titration width may be neglected according to eq 12, since the increment $\delta s_{CM}/2$ is only about half of the total charge density $s = s_{AM} + \delta s_{CM}/2$.

(23) "Handbook of Chemistry and Physics", 54th ed., 1974, p D-126.
(24) D. J. Shaw, "Introduction to Colloid and Surface Science", 2nd ed., Academic Press, London, 1970, p 135.
(25) P. Fromherz and B. Masters, *Biochim. Biophys. Acta*, **356**, 270 (1974).
(26) R. F. Chen, *Anal. Lett.*, **1**, 423 (1968).
(27) K. H. Drexhage in "Progress in Optics", Vol. XII, E. Wolf, Ed., Elsevier, Amsterdam, 1974.

Thus the actual value of the antenna pK is explained as follows: upshift from pK^{w} = 7.7 to pK^{i} = 8.8 by the location in the membrane, downshift to pK^{mw} = 5.2 by the positive matrix, upshift to pK^{mw} = 6.9 by three-valent counterions, and upshift to pK^{mw} = 7.4 by the negative charges of the pigment itself.

The range of the fluorescence drop shown in Figure 6 coincides with the pH range of matrix deprotonation. A pK^{mw}_{AM} = 8.8 in citrate is estimated with eq 4 considering the potential Ψ = +40 mV for semiprotonated amine with fully deprotonated pigment. The drop is not due to the reduction of electrical potential in the deprotonated matrix causing back-protonation of the pigment. The depression of fluorescence persists up to pH 12 where even for highly negatively charged films the dye dissociates completely.[25]

Deprotonation of the docosylamine matrix appears to affect the fluorescence yield of the pigment base. Since no drop is observed with low indicator density, a direct quenching by the amine is excluded. The effect must be assigned to an enhancement of pigment association in the neutral matrix with an enhanced concentration quenching. The observation indicates two-dimensional electrostatic solvation of the negatively charged dye base by the positive ammonium groups of the matrix which shields the chromophores from each other. The solvation shell is destroyed by deprotonation. The existence of such two-dimensional solvation of charged dyes by charged lipids is confirmed in mixed chromophore systems by energy transfer.[28]

C. Electrode. This section describes the characteristics of the semiconductor electrode, the location of the edge of conduction band as determined by capacitance, and the intrinsic photocurrent which forms the background of sensitization. The effect of pH is discussed in terms of an interfacial acid–base reaction.

1. Capacitance. The square of the reciprocal capacitance of the blank electrode increases linearly with potential above a threshold, shifted by −50 mV per pH unit, as shown in Figure 7a. C_{EL} may be expressed by the capacitance of the electrode/electrolyte interface (Helmholtz layer) C_H and of the space charge in the semiconductor (Schottky layer) according to eq 13.[29] This

$$C_{EL}^{-2} = C_{H}^{-2} + C_{SC}^{-2} \qquad (13)$$

relation holds if the partitioning of electrode potential between the Helmholtz and Schottky layer is considered,[29] such that C_{SC} in eq 13 is given by the Schottky–Mott relation for space charge capacitance and the difference $V - V_{FB}$ of the applied potential V and potential V_{FB} of vanishing space charge (flatband potential) according to eq 14, where ϵ is the permittivity of the electrode

$$C_{SC} = [(V - V_{FB} - \Phi_{th})/e\epsilon n/2]^{-1/2} \qquad (14)$$

and n is the density of donor states. The data of Figure 7a are fitted with $n = 7 \times 10^{19}$ cm^{-3}.

The constant shift of C_{EL}^{-2} (V) by −50 mV per pH unit reflects a shift of flatband potential according to eq 13 and 14. In the neutral pH range a linear relation $V_{FB} = V(\mathrm{pH})$ exists with $dV_{FB}/d\mathrm{pH}^{w} = -50$ mV and $d^2V_{FB}/d\mathrm{pH}^{w} = 0$. The change of flatband potential is caused by the pH dependence of the potential drop between the surface of the electrode and the electrolyte.

2. Intrinsic Photocurrent. The photocurrent across the electrode/electrolyte interface increases with applied potential as shown in Figure 7b. A shift by −50 mV per pH unit is observed. This current i_{SC} is caused by light absorption a_{SC} in the space charge and transfer of the holes produced across the interface with yield q_{tr} in competition with recombination with surface states (eq 15).[30]

$$i_{SC} = q_{tr}a_{SC} \qquad (15)$$

a_{SC} is obtained from the absorption coefficient of the electrode $\alpha_{SC} = 7 \times 10^{4}$ cm^{-1} [31] and the thickness of the space charge d_{SC} = ϵC_{SC}^{-1}. Considering that the rate of recombination is proportional to the number of occupied surface states and assuming an exponential distribution of surface states below the edge of the conduction band of width V_{ss}, q_{tr} is given by eq 16.[5,30]

$$q_{tr} = [1 + \exp(V_{HW}^{tr} - V)/V_{ss}]^{-1} \qquad (16)$$

The difference of the half-wave potential V_{HW}^{tr} and of V_{FB} is $V_{HW}^{tr} - V_{FB} = V_{ss} \ln (k_{re}^{FB}/k_{tr})$, where the rate constants refer to recombination at $V = V_{FB}$ and to hole transfer. The data of Figure 7b are fitted by eq 15 and 16 with V_{ss} = 150 mV and $k_{re}^{FB} = 120k_{tr}$. The shift of i_{SC} by −50 mV per pH unit indicates a shift of flatband potential with pH according to eq 15 and 16. This increment is consistent with that derived from capacitance data.

3. Helmholtz Potential and pH. A shift of flatband potential V_{FB}, i.e., a shift of potential drop Ψ between electrode and electrolyte by about $-2.3\Phi_{th}$ = −59 mV per pH unit, is common for oxidic semiconductors.[32] It is assigned generally to a dissociation of surface hydroxyls in the neutral pH range.[33-36] The quantitative interpretation of the effect, however, has not been unequivocal.

An evaluation of the experimental slope $-d\Psi/d\mathrm{pH} \equiv \Phi\mathrm{pH}$ = 50 mV must be based on eq 8. It depends crucially on the assumptions made on the nature of the electrical double layer, i.e.,

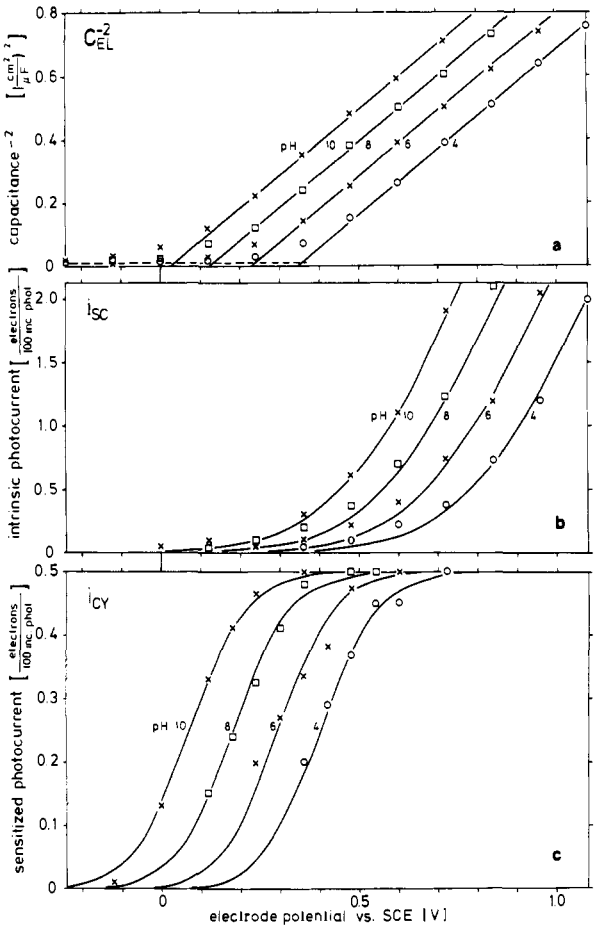

Figure 7. (a) Square of reciprocal capacitance of blank electrode C_{EL}^{-2}; (b) intrinsic photocurrent of electrode i_{SC}, illumination at 330 nm; (c) photocurrent sensitized by cyanine pigment i_{CY}, illumination 470 nm. All data as functions of electrode potential vs. SCE. (a) is fitted with eq 13 and 14; (b) with eq 15 and 16; (c) with eq 17 and 20.

(28) P. Fromherz, to be published.
(29) R. DeGryse, W. P. Gomes, and J. Vennick, *J. Electrochem. Soc.*, **122**, 711 (1975).
(30) R. H. Wilson, *J. Appl. Phys.*, **48**, 4292 (1971).
(31) H. Koestlin, R. Jost, and W. Lems, *Phys. Status Solidi*, **29**, 87 (1975).
(32) S. M. Ahmed in "Oxides and Oxide Films", Vol. 1, J. W. Diggle, Ed., New York, 1972, p 319.
(33) M. Hofmann-Perez and H. Gerischer, *Ber. Bunsenges. Phys. Chem.*, **65**, 771 (1961).
(34) P. J. Boddy and W. H. Brattain, *J. Electrochem. Soc.*, **110**, 570 (1963).
(35) H. Gerischer, M. Hofmann-Perez, and W. Mindt, *Ber. Bunsenges. Phys. Chem.*, **69**, 130 (1965).
(36) P. J. Boddy, *J. Electroanal. Chem.*, **10**, 199 (1965).

on $d\Phi/ds$ and on the state of dissociation b_{OH} of the surface.

Application of the Gouy–Chapman theory as for the charged membrane, i.e., insertion of eq 11 into eq 8, leads immediately to an inconsistency. Full success and complete failure of the Gouy–Chapman approach are apparent here in one physical system for two interfaces of different chemical nature.

If, as usual, the double layer is assumed to be of the Stern–Helmholtz type, eq 2 is a linear relation $\Psi = \Psi_0 + a_H^{-1}(s_0 + eb_{OH}n_{OH})$ with unknown $a_H = ds/d\Phi$. Considering that the experimental constance of dV_{FB}/dpH corresponds to a theoretical condition $d^2\Psi/dpH^2 = 0$, differentiation of eq 8 yields $b_{OH} = {}^1/_2$, and reinsertion of this result into eq 8 leads, with $n_{OH} = 5 \times 10^{-14}$ cm^{-2},[35] to $a_H = 0.14$ mF/cm^2. By computation of the complete function $\Psi(pH)$ with eq 1–4, a constant slope $d\Psi/dpH = -50$ mV is obtained over four pH units on both sides of the pH of semidissociation pK_{OH}^{mw}. It should be noted here that the double layer constant a_H has to be distinguished conceptually from the differential capacitance C_H of the Helmholtz layer. The latter refers to the total electrode/electrolyte interface and is quite unspecific in its value with respect to the chemical nature of the surface of semiconductors and metals.[35]

Whether the pK_{OH}^{mw} of interfacial stannate is indeed near neutrality can be estimated only roughly. Taking $pK_{OH}^{w} = 8.5$ as tabulated for germanate,[37] assuming a shift of 1 pH unit due to lower interfacial polarity, i.e., a $pK_{OH}^{i} = 9.5$, and calculating from eq 2 and 3 a potential $\Psi = -285$ mV due to the semidissociated hydroxyls, one obtains with eq 4 a value $pK_{OH}^{mw} = 14.5$, which is far from neutrality.

However, the pK_{OH}^{mw} may be shifted down to 7 if a positive contribution of $(\Psi_0 + a_H^{-1}s_0) = +430$ mV to the potential Ψ exists as caused by surface dipoles or adsorbed ions (eq 2 and 3). In that case the total potential for $b_{OH} = 0.5$ is $\Psi = +145$ mV which leads to $pK_{OH}^{mw} = 7$. As a matter of fact, the total potential drop between electrode and electrolyte with flat bands at pH 7 (Helmholtz potential) as estimated from work functions is positive and with +350 mV in the range postulated (Figure 2).

The straightforward evaluation of the pH-dependent flatband potential as presented does not lead to physical inconsistencies. It avoids arbitrary assumptions on the state of dissociation of the semiconductor surface and of the electrical double layer.[35,36]

D. Electron Injection. This section describes the photosensitization of the semiconductor by the membrane bound pigment. The quantum yield is assigned to the elementary processes involved. The basis of photocurrent change with potential and pH is discussed.

1. Quantum Yield and Mechanism. The cyanine pigment R gives rise to a spectral component of the photocurrent which agrees with the absorption of the dye (Figures 5 and 8). The sensitized current i_{CY} increases sigmoidal with applied potential as shown in Figure 7c. The saturation current is pH independent.

Spectral sensitization of semiconductor electrodes by adsorbed dyes has been studied by several authors.[38-40] i_{CY} depends on the absorption of the pigment a_{CY}, the yield of electron transfer to the surface of the semiconductor q_{el}, and the yield of electron release from the intermediate $R^+e_i^-$ (R^+ oxidized pigment, e_i^- interfacial electron) to the bulk of the electrode, q_{rel}, according to eq 17 (cf. Figure 2).[5]

$$i_{CY} = q_{rel}q_{el}a_{CY} = q_{rem}q_iq_{el}a_{CY} \quad (17)$$

According to Figures 5 and 7c the quantum yield of current in saturation is about $i_{CY}/a_{CY} = q_{CY} = 0.2$. It has to be assigned to q_{rel} or to q_{el} or to both. q_{el} may be estimated from fluorescence quenching caused by the electrode since electron transfer is the only decay process induced by the semiconductor.[5] The result is $q_{el} > 0.95$, which indicates that deactivation processes within the pigment may be neglected. The loss in $q_{CY} = 0.2$ has to be attributed to unproductive deactivation after electron transfer in the intermediate state $R^+e_i^-$ (cf. Figure 2).

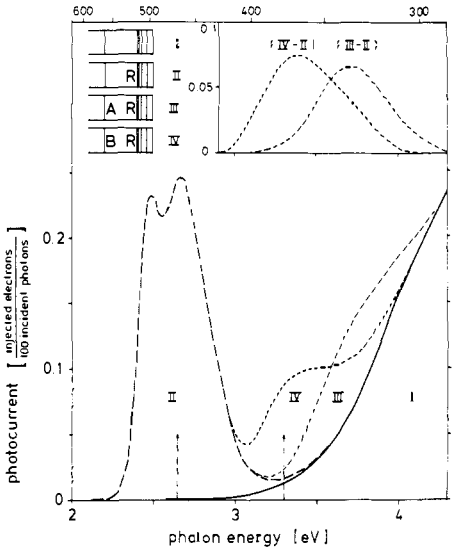

Figure 8. Action spectra of photocurrent: semiconductor electrode (I) with docosylamine bilayer matrix; (II) with reaction pigment (cyanine); (III) with reaction pigment and antenna pigment (coumarin), pH 5; and (IV) with reaction pigment and antenna pH 9. The spectra are measured near half-wave potential of sensitized current under constant-field condition. The increment of the antenna i_{CM} is shown in the insert. Excitation energy for cyanine and coumarin during pH titration is indicated by arrows.

The only process competing with electron release at high potentials is recombination. The fact that the current saturates at a yield below 1 indicates that charge release even with strong electric fields in the space charge cannot compete with all recombination processes. Within a kinetic scheme this observation leads to the conclusion that the primary interfacial state of the transferred electron is not sensitive to the space charge, which is reached only in a second interfacial transition with a yield in saturation of $\bar{q}_i = 0.2$. It is this second interfacial state where the electron is removed by the field with yield $\bar{q}_{rem} = 1$ in saturation (Figure 2 and eq 17). Structural assignment of the two kinetic interfacial electronic states is not attempted. With eq 18 the rate of recombination k_{rec} is found to be five times faster than the interfacial transition rate k_i.

$$\bar{q}_i = [1 + k_{rec}/k_i]^{-1} \quad (18)$$

Regeneration of the pigment by an external reductant (thiourea) does not enter these kinetic considerations, which refer to the very beginning of illumination, where bleaching is irrelevant.[6] Supersensitization, i.e., reduction of oxidized dye in the intermediate $R^+e_i^-$ with subsequent induced release of the electron[5] plays a minor role in the present membrane assembly. Current enhancement in saturation by thiourea is only 5%.

2. Half-Wave Potential. The sensitized current drops at low potential within 300 mV to zero. The half-wave potential is shifted by −50 mV per pH unit. As the electron transfer step is independent on the applied potential,[5] this current drop may be due (a) to an enhancement of back-donation of electrons from occupied surface states to R^+ in $R^+e_i^-$ (rate constant k_b) lowering q_i,[5] and (b) to a slowing down of charge removal from $R^+e_i^-$ (rate constant k_{rem}) in the weaker space charge lowering q_{rem}.[19]

Assuming that the rate of back-donation is proportional to all occupied surface states (cf. section C.2), q_i depends on potential according to eq 19. The difference of half-wave potential V_{HW}^b

$$q_i = \bar{q}_i\,[1 + \exp(V_{HW}^b - V)/V_{ss}]^{-1} \quad (19)$$

and of V_{FB} is $V_{HW}^b - V_{FB} = V_{ss} \ln [k_b^{FB}/(k_{rec} + k_i)]$ with $k_b^{FB} = k_b(V_{FB})$. With $V_{ss} = 150$ mV the width of current drop becomes $4V_{ss} = 600$ mV.[5] This width differs significantly from the experimental value of 300 mV (Figure 7c). An assignment of the

(37) Reference 23, p D-130.
(38) H. Gerischer and H. Tributsch, *Ber. Bunsenges. Phys. Chem.*, **72**, 437 (1968).
(39) K. Hauffe, H. Pusch, and J. Range, *Z. Phys. Chem.* (*Frankfurt am Main*), **64**, 122 (1969).
(40) H. Tributsch and M. Calvin, *Photochem. Photobiol.*, **14**, 95 (1971).

observed current drop exclusively to an enhancement of back-donation is unlikely. The field-dependent rate constant of charge removal k_{rem} has to be taken into account.

The experimental data (Figure 7c) are described by assuming an exponential dependence of k_{rem} on the potential drop $(V - V_{FB})$ in the space charge, i.e., $k_{rem} = k_{rem}^{FB} \exp[\beta(V - V_{FB})/\Phi_{th}]$ with $k_{rem}^{FB} = k_{rem}(V_{FB})$. Then q_{rem} is expressed by

$$q_{rem} = [1 + \exp\beta(V_{HW}^{rem} - V)/\Phi_{th}]^{-1} \quad (20)$$

The difference of half-wave potential V_{HW}^{rem} and of V_{FB} is $V_{HW}^{rem} - V_{FB} = (\Phi_{th}/\beta) \ln (k_{rec}/k_{rem}^{FB})$. Fit of the data is obtained with $k_{rec} = 2.7k_{rem}^{FB}$ and a weighting factor $\beta = 0.35$. With this relation the pH dependence of sensitization is assigned quantitatively to the pH dependence of the flatband potential, i.e., to the shift of the band structure by the pH-dependent Helmholtz potential. A mechanistic interpretation of the form of eq 20 is not attempted.

E. pH Modulation of Sequential Energy and Electron Transfer. This section describes energy transfer from the excited antenna pigment to the reaction center of electron transfer, the spectral sensitization of photocurrent as due to sequential transfer of energy and electron, and finally the chemical modulation of this current by pH titration of the antenna, i.e., the complete device.

1. Energy Transfer. The fluorescence spectrum of the antenna and the absorption spectrum of the reaction pigment overlap perfectly as shown in Figure 5. The efficiency of energy transfer q_{en} is obtained from quenching of fluorescence intensity as induced by the acceptor according to eq 21, where I and I_0 are the in-

$$I/I_0 = 1 - q_{en} \quad (21)$$

tensities with and without acceptor. With $I/I_0 = 0.5$ (cf. Figure 6) one obtains $q_{en} = 0.5$.

This value may be compared with the formula for dipole–dipole coupled energy transfer between thermally relaxed donor–acceptor layers (eq 22).[2,41] q_{CM}^0 is the yield of fluorescence of the antenna

$$\gamma\left(\frac{\lambda_f/2\pi}{nd}\right)^4 a_{CY} q_{CM}^0 \int d\lambda \alpha_{CY}\varphi_{CM} = \frac{q_{en}}{1 - q_{en}} \quad (22)$$

without acceptor, a_{CY} is the maximum absorption of the cyanine, $\alpha_{CY}(\lambda)$ is the relative absorption spectrum, $\varphi_{CM}(\lambda) = f(\lambda)(\lambda/\lambda_f)^4$ ($f(\lambda)$ = normalized fluorescence spectrum, λ_f = wavelength of fluorescence maximum), n is the refractive index of the medium, and d is the distance of donor and acceptor layer. The constant $\gamma = 0.144$ refers to random orientation of donor and acceptor moments in the plane of the membrane.[41]

For an exact evaluation of electromagnetic energy transfer, the multilayered optical nature of the glass/tin oxide/paraffin/water assembly should be considered. Evaluation of true absorption and of energy transfer amplitude in such a system is not described in the literature.[27,41-43] A detailed investigation of the problem is beyond the scope of the present paper.[44] For an estimate, eq 22 for a homogeneous isotropic medium with $n = 1.56$,[45] $d = 6$ nm,[22] and the measured $a_{CY} = 0.022$ (Figure 5) is applied. With the spectral data of Figure 5 the overlap correction is $\int d\lambda \alpha_{CY}\varphi_{CM} = 0.75$. (This factor is omitted in ref 6.) Coincidence with the experimental q_{en} is obtained by eq 22 with $q_{CM}^0 = 0.1$. The low value, as compared to the well-known high quantum yield of coumarins,[46] is due to concentration quenching in the highly doped membrane.

2. Sequential Energy and Electron Transfer. The total photocurrent in the antenna system is due to electron-hole production in the semiconductor (eq 15), to direct excitation of the reaction pigment by external light with electron injection (eq 17), and to the antenna excitation with subsequent energy transfer and electron injection according to eq 23. The three components are

$$i_{tot} = i_{SC} + i_{CY} + i_{CM} \quad (23)$$

apparent in the photocurrent spectrum of Figure 8. The spectrum of sequential energy–electron transfer as obtained after subtraction of the other two components is shown in the upper right corner of Figure 8. The action spectra for the two pH values correspond closely to the absorption spectra of the antenna (Figure 5). With $a_{CM} = 0.014$ the yield of the two-step sensitized current is about $q_{CM} = i_{CM}/a_{CM} = 0.05$.

The current sensitized by the antenna is determined by a product of quantum yields (eq 24). With $q_{en} = 0.5$, $q_{el} = 1$, and

$$i_{CM} = q_{rem}q_i q_{el} q_{en} a_{CM} \quad (24)$$

$q_{rem}q_i = 0.1$ under the half-wave conditions chosen (cf. Figures 5 and 8), one obtains from eq 24 an antenna yield $q_{CM} = 0.05$ in good agreement with the experimental value. The coincidence indicates that sequential energy–electron transfer is a correct assignment of the observations. For control the reaction pigment has been removed from the assembly. In that case the spectral component of the antenna is less than 5% of the complete system.

3. pH Modulation at Constant Field. The absorption of an antenna layer following an ideal titration is given by eq 25 where

$$a_{CM} = \frac{a_B + a_A \exp[2.3(pK_{CM}^{mw} - pH^w)]}{1 + \exp[2.3(pK_{CM}^{mw} - pH^w)]} \quad (25)$$

a_A and a_B are the absorption for pure acid and base. Choosing an excitation energy of 3.3 eV, only the base of the coumarin contributes to light absorption (Figure 5) such that the antenna current in eq 23 and 24 is modulated by pH according to a simple titration curve.

The total photocurrent, however, reflects this titration only if according to eq 23 and 24 the yield of electron injection and the background of intrinsic photocurrent at the wavelength of base excitation are pH independent.

As shown in Figure 7c the quantum yield of electron injection is independent of pH in the saturation range at high potential.

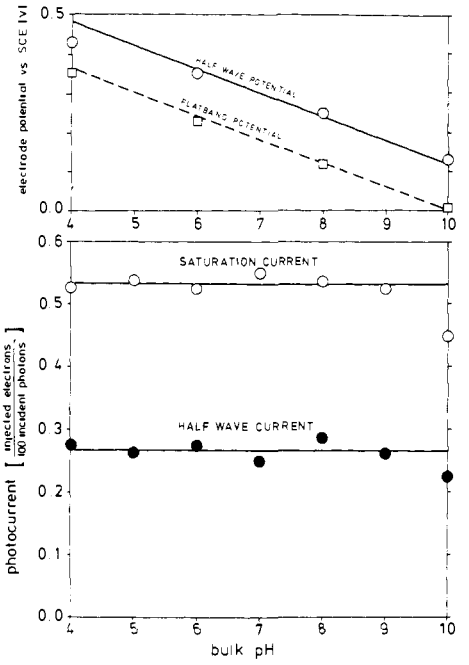

Figure 9. Sensitized photocurrent of complete antenna assembly with illumination of reaction pigment (470 nm) under constant-field condition in the space charge as a function of pH. The open circles refer to the saturation range 480 mV above flatband potential, the filled circles to half-wave potential 120 mV above flatband potential. The compensation potentials applied are indicated by the full line in the upper part of the figure (slope −60 mV per pH unit). Measured half-wave and flatband potentials are marked for comparison.

(41) H. Kuhn, *J. Chem. Phys.*, **53**, 101 (1970).
(42) K. H. Tews, *Ann. Phys.*, **29**, 97 (1973).
(43) R. R. Chance, A. Prock, and R. Silbey, *Adv. Chem. Phys.*, **37**, 1 (1978).
(44) P. Fromherz, to be published.
(45) J. D. Swalen, K. E. Rickhoff, and M. Tacke, *Opt. Commun.*, **24**, 146 (1978).
(46) K. H. Drexhage in "Dye Lasers", F. P. Schaefer, Ed., Springer, Berlin, 1973, p 144.

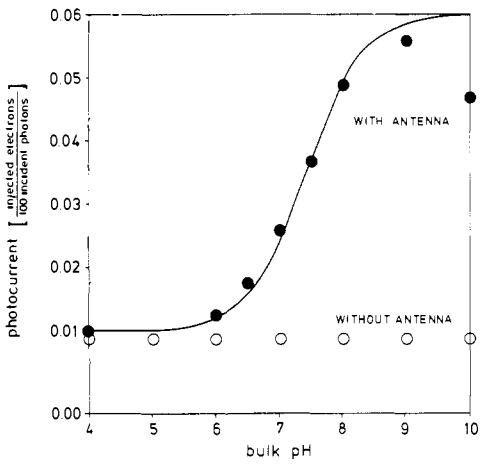

Figure 10. Sensitized photocurrent of complete antenna assembly with illumination of antenna pigment (380 nm) under constant-field condition in the space charge as a function of pH. The data are fitted by an ideal titration curve with a pK taken from fluorescence titration of the antenna (Figure 6). The circles indicate the background in a system without antenna.

However, in that potential range the intrinsic photocurrent is strongly pH dependent, as shown in Figure 7b for a wavelength of 330 nm. At the wavelength of antenna excitation, 380 nm, this current is lower (Figure 8), but still of the same order as the antenna-sensitized current.

The interference of antenna and background could be bypassed by a pigment system with energies far from the band edge. However, an antenna dye which matches all the other requirements of the device (pK near neutrality, steep titration curve, high quantum yield of fluorescence, and high absorbance at the longer wavelength) is not available at the present moment.

The background current may be suppressed by applying a lower electrode potential (Figure 7b). In that potential range, however, a strong pH dependence of the electron injection current appears (Figure 7c), which is due to the changing yield of charge removal as modulated by the pH-dependent Helmholtz layer (eq 20). In order to titrate the device with constant yield q_{rel}, the field in the space charge has to be held pH invariant.

This constant-field condition is realized by following the pH change of the Helmholtz potential with the external potential, such that the bands are held at constant slope (Figure 2). Since the Helmholtz potential changes constantly by about -59 mV per pH unit, this procedure may be realized without fit during the titration. Figure 9 shows the result of a constant-field titration near the half-wave potential of the injection current. The circles refer to the saturation current 480 mV about the flatband potential, observed at 470 nm with the complete assembly. The dots show the half-wave current 120 mV above V_{FB}. Perfect compensation of the pH influence is achieved. On top of Figure 9 the standard potential/pH line of -60 mV per pH unit used for compensation is compared to the measured flatband and half-wave potentials. Such a standard line is used since the actual slope varies somewhat from batch to batch.

Under these constant-field conditions the photocurrent with excitation of the antenna at 380 nm is shown in Figure 10 as a function of pH. The data are fitted according to eq 23-25 by an ideal titration curve for i_{CM} with pK = 7.4 as taken from antenna fluorescence of Figure 6 and a constant background i_{SC}. Perfect agreement of fluorescence and photocurrent titration is apparent.

This is the realization of sequential energy-electron transfer modulated by protons. The switching experiment shown in Figure 3 is made under identical conditions. The chemical nature of the coumarin pigment is imprinted onto the electrical response of the semiconductor by sequential energy and electron transfer.

An Empirical Valence Bond Approach for Comparing Reactions in Solutions and in Enzymes

Arieh Warshel* and Robert M. Weiss

Contribution from the Department of Chemistry, University of Southern California, Los Angeles, California 90007. *Received March 3, 1980*

Abstract: A simple and reliable empirical valence bond (EVB) approach for comparing potential surfaces of reaction in solution and in enzymes is developed. The method uses the valence bond concept of ionic-covalent resonance to obtain a Hamiltonian for the isolated molecule and then evaluates the Hamiltonian for the reaction in solution by adding the calculated solvation energies to the diagonal matrix elements of the ionic resonance forms. The resulting potential surface is then calibrated by using pK_a measurements and other information about the reaction in solution. The calibrated potential surface provides a simple tool for comparing the activation energy of a reaction in solution with that in an enzyme by replacing the solvation energies of the ionic resonance forms by their interactions with the enzyme active site. The EVB method is illustrated by calculations of typical solution reactions including an ionic bond-breaking reaction, a proton-transfer reaction, and a general-acid catalysis reaction. The application of the EVB method to studies of enzymic reactions is demonstrated by calculating the potential surface for the rate-limiting step of the catalytic reaction of lysozyme and comparing the calculated activation energy to that of the reaction in solution.

I. Introduction

It is known that the environment in which a reaction occurs can influence the reaction rate profoundly. Large rate enhancements have been observed upon increasing solvent polarity (see for example, ref 1). This is particularly true for a large class of bond-breaking and -forming reactions that pass through ionic or partially ionic transition states. Thus, it is important to develop a theoretical method able to compare potential surfaces of these reactions as the environment is changed.

Early in the development of quantum chemistry considerable progress was made with the valence bond picture of chemical bonding, but the approach was largely abandoned during the last 30 years for molecular orbital methods. These methods (which are much simpler than valence bond to implement in ab initio approaches) have had considerable success in many areas but have

(1) Wiberg, K. B. "Physical Organic Chemistry"; Wiley: New York, 1963.

0002-7863/80/1502-6218$01.00/0